Li, YL., Ge, ZM., Xie, LN. et al. Effects of waterlogging and elevated salinity on the allocation of photosynthetic carbon in estuarine tidal marsh: a mesocosm experiment. Plant Soil (2022).

1 **TITLE: Effects of waterlogging and elevated salinity on the allocation of photosynthetic**

2   **carbon in estuarine tidal marsh: an mesocosm experiment**

3

4 **AUTHORS:** Ya-Lei Li[1,2,3], Zhen-Ming Ge[1,2,*], Li-Na Xie[1,3], Shi-Hua Li[1], Li-Shan Tan[1], Kasper

5   Hancke[3]

6 **INSTITUTES:**

7 [1] *State Key Laboratory of Estuarine and Coastal Research, Institute of Eco-Chongming, Center*

8   *for Blue Carbon Science and Technology, East China Normal University, Shanghai, China*

9 [2] *Yangtze Delta Estuarine Wetland Ecosystem Observation and Research Station, Ministry of*

10   *Education & Shanghai Science and Technology Committee, Shanghai, China*

11 [3] *Section for Marine Biology, Norwegian Institute for Water Research (NIVA), Oslo, Norway*

12

13 *** CORRESPONDING AUTHOR**

14 *E-mail address*: zmge@sklec.ecnu.edu.cn

15 Address: Estuary & Coast building, 500 Dongchuan Road, 200241 Shanghai, China

16

17 **ABSTRACT**

18 **Background and aim**

19 Coastal marshes and wetlands hosting blue carbon ecosystems have shown vulnerability to sea-

20 level rise (SLR) and its consequent effects. In this study, we explored the effects of

21 waterlogging and elevated salinity on the accumulation and allocation of photosynthetic carbon

22 (C) in a widely distributed species in marsh lands.

23 **Methods**

24 The plant–soil mesocosms of *Phragmites australis* were grown under waterlogging and

25 elevated salinity conditions to investigate the responses of photosynthetic C allocation in

26 different C pools (plant organs and soils) based on $^{13}CO_2$ pulse-labeling technology.

27 **Results**

28 Both waterlogging and elevated salinity treatments decreased photosynthetic C fixation. The

29 hydrological treatments also reduced ^{13}C transport to the plant organs of *P. australis* while

30 significantly increased ^{13}C allocation percentage in roots. Waterlogging and low salinity had no

31 significant effects on ^{13}C allocation to rhizosphere soils, while high salinity (15 and 30 ppt)

32 significantly reduced ^{13}C allocation to soils, indicating a decreased root C export in saline

33 environments. Waterlogging enhanced the effects of salinity on the ^{13}C allocation pattern,

34 particularly during the late growing season. The responses of flooding and elevated salinity on

35 C allocation in plant organs and rhizosphere soils can be related to changes in nutrient, ionic

36 concentrations and microbial biomass.

37 **Conclusion**

38 The adaptation strategy of *P. australis* led to increased C allocation in belowground organs

39   under changed hydrology. Expected global SLR projection might decrease total C stocks in *P.*

40   *australis* and alter the C allocation pattern in marsh plant-soil systems, due to amplified effects

41   of flooding and elevated salinities.

42

43   **Key words:** Coastal wetland; Photosynthetic carbon; Carbon allocation; Sea-level rise; Soil

44   biochemistry

45

INTRODUCTION

Coastal salt marshes play a notable role in sequestering carbon (C) in plants and soils and are included under the term "blue carbon" ecosystems (Mcleod et al. 2011). These ecological important coastal ecosystems have shown vulnerability to global climate change (Kirwan and Mudd 2012; Xin et al 2022). Based on the 6th assessment report by the Intergovernmental Panel on Climate Change (IPCC), global warming will lead to a mean sea level rise by 0.43 to 0.84 meters by 2100 (medium confidence) relative to the years 1986–2005 (IPCC 2019). Sea-level rise (SLR) would cause frequent prolonged inundation and saltwater intrusion in coastal wetlands (Neubauer et al. 2013).

Carbon uptake by plants (photosynthesis) and its allocation in plant organs and soils are essential to wetlands ecosystems and their carbon storage and sequestration capacity (Alongi 2012). Expected SLR projections are likely to alter plant photosynthesis and the allocation of photosynthetic C between different internal and external plant C pools, thus potentially affecting the C balance of coastal ecosystems (Luo et al. 2009). The response of plant photosynthesis to different environmental stresses (i.e., increased inundation and elevated salinity) in coastal wetlands has been addressed widely (Pezeshki and DeLaune 1997; Li et al. 2018; Li et al. 2020). The ratio of root to shoot mass (root:shoot ratio) is a measurement method and is frequently employed to capture carbon and biomass allocation in plants (Poorter et al. 2012) or investigate the investment and allocation of photosynthates between above- and belowground organs (Titlyanova et al. 1999). Recently, *in situ* ^{13}C (or ^{14}C) pulse-labeling technology has been applied to trace the flow of newly assimilated C and its allocation into different carbon pools (Simard et al. 1997; Ge et al. 2012; Zhang et al. 2017). This technology

68   has been adopted to quantify the C allocation and translocation of marsh plants in response to

69   environmental changes (Soetaert et al. 2004; Wersal et al. 2013).

70   Prolonged waterlogging has been shown to decrease photosynthesis in marsh land plants

71   through damaging the photosynthetic apparatus (Mauchamp and Méthy 2004) or inhibiting its

72   photosynthetic activity (Li et al. 2018), thus potentially influencing the allocation of assimilates

73   among C pools. The effects of waterlogging on C allocation in coastal plants are however not

74   fully constrained. Some studies have shown that waterlogging increases photosynthetic C

75   allocated to belowground plant biomass of mangroves (Pezeshki et al. 1997) and marshes

76   (Minden et al. 2012), whereas Naidoo and Naidoo (1992) showed the opposite pattern in marsh

77   plants. Other studies have reported on neutral response of C allocation in plant biomass to

78   increased inundation in marshes (Xue et al. 2018). Several studies of inland wetlands (i.e.,

79   paddy and sedge wetlands) have shown lower C exudation from plant roots into soils (Tian et

80   al. 2013) or unaffected C allocation (Kotas et al. 2019). Nevertheless, C allocation in plants and

81   soils (or rhizodeposition) systems impacted by changing hydrology conditions is understudied

82   in coastal wetlands.

83   Sea level rise would increase the frequency and duration of saltwater intrusion to wetland

84   and marsh and lead to increased salinity in coastal areas (Neubauer et al. 2013). Elevated

85   salinity, like waterlogging, might affect the allocation of photosynthetic assimilates among

86   different C pools in marsh plants due to plant's adaptation strategies to environmental changes

87   (Soetaert et al. 2004; Li et al. 2016). For instance, plants may favor C allocation to storage and

88   defense of above organs for long-term survival (Wang et al. 2019a). Soetaert et al. (2004)

89   compared two reed beds with different salinity levels and found that a higher proportion of

90   photosynthetic carbon flowed back toward the rhizome-root system in a mesohaline marsh than

91   in an oligohaline marsh. Some studies on root:shoot ratios of marsh plants showed that the ratio

92   increased with elevated salinity (Lissner et al. 1999; Scarton et al. 2002; Xue et al. 2018; Tang

93   et al. 2021), suggesting more investment of photosynthates into belowground parts. However,

94   Li et al. (2016) reported a contradictory result, showing that a lower percentage of assimilated

95   C in plant roots occurred under high salinity than under low salinity. This altered C allocation

96   pattern potentially affects photosynthetic C allocation between plant and soil pools, which was

97   supported by observations in pot experiments showing lower soil organic C content under high-

98   salinity treatments of marsh soil (Li et al., 2016).

99   However, how photosynthetic C allocation in the plant and soil systems responds to

100   changes in combined flooding and salinity projected by SLR conditions is poorly understood

101   for coastal wetlands. Here we present the results of a mesocosm experiment with the plant–soil

102   systems of *Phragmites australis* (known as the common reed) subjected to waterlogging and

103   elevated salinity treatments. *P. australis*, an herbaceous perennial grass, is a widely distributed

104   marsh species globally, covering approximately half of the coastal marsh area in China. The

105   objective of this study was to quantify photosynthetic C allocation within plants and their

106   translocation into the soil in coastal marsh ecosystems as a response to flooding and elevated

107   salinity, and the combined effect. We applied a $^{13}CO_2$ pulse-labeling approach and tracked the

108   allocation of ^{13}C in different C pools in the *P. australis* plant–soil system during the growing

109   season.

110

111

MATERIALS AND METHODS

Mesocosm experiment setup

In the Yangtze River Estuary of East China, a plant-soil mesocosm system was prepared by collecting intact plant-soil blocks from a coastal oligohaline marsh in the Chongming Dongtan wetland (31°25′-31°38′N, 121°50′-122°05′E). The sampling site had annual average surface water and soil salinities of 3 to 5 ppt and 1500 to 2000 mg L^{-1}, respectively (Li et al. 2020). The wetland has a maritime monsoon climate with an average annual temperature of 15.3°C and an average annual rainfall of 1 022 mm. The tides are characterized by irregular shallow sea half-day tides with a maximum tide height of 4.62 to 5.95 m over many years and an average annual tide height of 1.96 to 3.08 m (Ge et al. 2008).

The intertidal zone is dominated by the common marshland species *P. australis* which was sampled for the mesocosm experiments from the same tidal line. In December (winter) of 2016, a total of 32 intact plant-soil monoliths were excavated after stem senescence. The above dead stems were removed and then each soil monolith was put into a polyethylene box (L 32 cm, W 24 cm, H 40 cm) for incubation. The small gaps between the soil block and the incubator were filled with soil materials collected near the sampling zone. A drain pipe with valve was installed in the bottom of each container to control the water level.

During January–February 2017, the mesocosms were watered and drained daily with freshwater to homogenize the soil salinity, which also allowed the samples two months of recovery from disturbance before starting the experimental treatments. When the plants began to germinate in early March, each mesocosm was fertilized with identical concentrations of Hoagland's nutrient solution (Hoagland and Arnon 1950). Over the entire growing season, the

134   period from January to November 32 mesocosms were established under even condition in a

135   naturally sheltered space under a transparent shelter that blocked rain. The shelter made of

136   plastic film has relatively high (~75%) transparency for visible light. During the cultivation

137   period of 2017, the daily atmospheric temperature (T_a) in the shelter was 25.7±4.9°C.

138   Following the methods applied by Li et al. (2020, 2022), *P. australis* were grown under

139   two waterlogging treatments; the waterlogging group (the water level was maintained at ~15

140   cm above the soil surface) and the non-waterlogging group functioning as control (the water

141   level was maintained at half of the container height, water level at 15–20 cm below the soil

142   surface). For each waterlogging group, four salinity treatments (using NaCl solution) were

143   installed consisting of three salinity levels (5, 15, and 30 ppt) and one freshwater-treated group

144   (control group, 0 ppt). Tap water which had been aerated for 24 h to remove the residual

145   chlorine was used to prepare both waterlogging and salinity treatment regimes. In total, eight

146   treatment regimes were prepared for the plant-soil mesocosms (2 water levels × 4 salinity

147   levels). In the factorial design, each treatment had four replicated incubators. Every two weeks

148   all mesocosms were drained for renewing irrigation. During the non-irrigation period,

149   freshwater was used to maintain the water level and to avoid excess salt accumulation from

150   water evaporation.

151

152   *¹³C pulse-chase labeling*

153   After the germination time (early May), number of *P. australis* shoots were stable at ~40 to 50

154   plants in each container, that was then the ^{13}C-CO_2 pulse labeling procedure was conducted.

155   Twenty-four mesocosms (2 water levels × 4 salinity levels × 3 duplicates) were used for the ^{13}C

156   pulse labeling and the remaining 8 mesocosms were used as unlabeled groups with maintained

157   natural ^{13}C background abundance. We first made 24 gastight marking chambers (1.75-m height

158   and effective size of planting container) constructed with plexiglass, and after each chamber

159   was fitted with two rubber tubes and four electric fans on the wall and a water-sealing slot on

160   the bottom.

161   Following Ge et al. (2012), the ^{13}C-CO_2 tracer (99.9 atom %^{13}C, Wuhan Newradar Special

162   Gas Co., Ltd., Wuhan, China) was applied with syringes connected to a three-way valve

163   between a high-pressure $^{13}CO_2$ cylinder and the marking chamber. An infrared gas analyzer (Li-

164   6400XT-40; Li-Cor Inc., Lincoln, NE, USA) was connected to the marking chamber to monitor

165   the total CO_2 concentration in the marking chamber. An air pump in the analyzer also controlled

166   the flow speed for $^{13}CO_2$ gas renewal. Ice packs were placed inside the chamber to avoid

167   elevated temperature.

168   On a sunny day in mid-May the ^{13}C-CO_2 pulse labeling was carried out from 7:30 to 12:30,

169   lasting 5 hours. During the half-hour before labeling began CO_2-free artificial mixed air (high-

170   purity gas N_2 + O_2) was used to flush the labeling room to avoid the interference of existing

171    $^{13}CO_2$ in the air. The CO_2 concentration in the chamber was maintained at 1000±100 ppm. To

172   minimize the potential effects of back diffusion of $^{13}CO_2$ from the soil and subsequent

173   photosynthetic uptake, we ventilated the greenhouse with fans and opened windows for 2 h

174   after labeling. The joints between containers and marking chambers were water-sealed to ensure

175   airtightness.

176

177   ***Sampling of plant and soil materials after labeling***

178   After ^{13}C-CO$_2$ marking labeled and unlabeled plants were periodically sampled at Day 0 (5

179   hours after labeling), and subsequently at Day 1, 3, 96, and 150. At each sampling time, five

180   medium-sized shoots were randomly selected and carefully dug out from each container. A steel

181   corer with an inner diameter of 2 cm was used to extract the soil samples (40-cm depth up to

182   the bottom of the container) from each clipped shoot, and two soil cores were taken for

183   belowground biomass and element measurements. Rhizosphere soil was carefully collected

184   within 1 cm of the root system. The plant samples were first separated into leaves, stems, and

185   roots and then cleaned with deionized water. All the sampled plant organs and soils were placed

186   in a ventilated oven at 105 °C for 30 min for fixation and then dried at 60 °C to constant weight.

187   The biomasses of leaves, stems, and roots per plant were weighed and recorded separately. Each

188   part of the plant organ was cut into pieces and stored in zip-lock bags for subsequent δ^{13}C

189   analysis. Soil samples were freeze-dried, finely ground in a mill, and stored in zip-lock bags

190   for subsequent δ^{13}C analysis.

191

192   ***Measurements of aboveground respiration***

193   Li et al. (2020) determined the photosynthetic rates under waterlogging and elevated salinity

194   treatments and these data were applied here. In addition to these, we in this study measured the

195   respired CO$_2$-^{13}C by shoots before shoot sampling according to Kutzbach et al. (2004). At Day

196   1, 3, 96, and 150, *P. australis* shoots were enwrapped by a black polyethylene columnar bag

197   from top to bottom. The bottom opening of the bag was tied around the base of shoot by a soft

198   steel clamp for bag seal. A sampling port with a three-way valve was installed on the

199   polyethylene bag ~50 to 75 cm above the soil surface. Ambient air was filled into the bags by

using an air pump, after which (~30 min) a 50-mL sample of gas was retrieved with a syringe

and injected into Fluode gas sampling bags. At the same time, ambient air was collected to

access the background $^{13}CO_2$ concentration.

$^{13}CO_2$ concentrations in the Fluode gas sampling bags ($[^{13}CO_2]_{sample}$) and background value

($[^{13}CO_2]_{ambient}$) were determined using the Piccaro Cavity Ringdown Spectrometer G2201-i

isotopic CO_2/CH_4 (Picarro Inc., Santa Clara, CA, USA). Then the respired CO_2-^{13}C (µg ^{13}C h^{-1}

plant^{-1}) by shoot in each mesocosm was calculated as follows,

$$R_{shoot}\text{-}^{13}C = \frac{1000([^{13}CO_2]_{sample}-[^{13}CO_2]_{ambient}) \times V_{sample} \times M}{V_m \times t_{sample}} \qquad (1)$$

where R_{shoot}-^{13}C is the respired CO_2-^{13}C by aboveground shoots (µg ^{13}C h^{-1} plant^{-1}), $[^{13}CO_2]$ is

the $^{13}CO_2$ concentration (ppm), V_{sample} is the effective volume of polyethylene bag (m^3), M is

the molar mass of ^{13}C (13 g mol^{-1}), V_m is the molar volume of CO_2 gas at 1 atmosphere of

pressure (22.41 L mol^{-1}), t_{sample} is the sampling duration (0.5 h).

^{13}C index calculations

The determination of C and $\delta^{13}C$ content in plant and soil samples was performed by the Flash

2000 EA-HT Elemental Analyzer (Thermo Fisher Scientific, USA) and Delta V Isotope Ratio

Mass Spectrometer (Thermo Fisher Scientific, Waltham, MA, USA). Carbon isotope ratios

were presented as $\delta^{13}C$. The $\delta^{13}C$ value was determined and expressed in ‰, relative to the Pee

Dee Belemnite (PDB) from a rock of Cretaceous age in Carolina (USA) (Moodley et al. 2000):

222 $$\delta^{13}C = \frac{R_{sample}-R_{PDB}}{R_{PDB}} \times 1000 \qquad (2)$$

223

224 where R_{sample} is the $^{13}C/^{12}C$ atomic ratio of the sample, the $R_{PDB} = 0.0112372$ is the $^{13}C/^{12}C$ ratio

225 of international standard (PeeDee Belemnite-PDB).

226   The photosynthate ^{13}C assimilation fixed in plants was expressed as the relative increase

227 in labeled sample relative to that of unlabeled (control) sample. Fixed ^{13}C by *P. australis*

228 photosynthesis can enter leaf, stem, root, and soils. The amount of fixed ^{13}C for the plant organs

229 was calculated as follows (Leake et al. 2006),

230

231 $$^{13}C_i = C_i \times \frac{(F_l-F_{nl})}{100} \times 1000 \qquad (3)$$

232

233 where C_i was net photosynthate ^{13}C assimilation of each component (g), F_l is the abundance

234 (%) of the labeled component ^{13}C, F_{nl} is the abundance (%) of the non-labeled component ^{13}C.

235 Then the ^{13}C abundance (F) can be calculated as follows (Lu et al. 2002a),

236

237 $$F = C_i \times \frac{(\delta^{13}C+1000) \times R_{PDB}}{(\delta^{13}C+1000) \times R_{PDB}+1} \times 100 \qquad (4)$$

238

239   The percentage of ^{13}C allocated into different plant organs ($^{13}C_{organ}\%$) of the leaves ($^{13}C_L\%$),

240 stems ($^{13}C_S\%$) and roots ($^{13}C_R\%$) can be calculated as:

241

242 $$^{13}C_{organ}\% = \frac{^{13}C_{organ}}{^{13}C_L+{}^{13}C_S+{}^{13}C_R} \times 100\% \qquad (5)$$

243

244   where C_{organ} pool is the carbon accumulation in the different plant organs of leaf (C_l), stem (C_s)

245   and root (C_r) of *P. australis*. $^{13}C_L$, $^{13}C_S$, and $^{13}C_R$ were the net photosynthate ^{13}C assimilated in

246   the plant organs of leaf, stem and root, respectively.

247

248   ***Measurement of soil variables***

249   At the end of the growing season (November) of 2017 the soil cores (40 cm depth, up to the

250   bottom of container) were excavated from each mesocosm for assessment of soil

251   physicochemical variables. All the roots were eliminated by squeezing the moist soil to pass

252   through a 2 mm sieve. The root-free soils from each container were mixed and air-dried. Then,

253   the soil sample was ground into a powder and sieved by a 1 mm sieve. Available nitrogen (AN)

254   was determined using the alkaline hydrolysis diffusion method, and available phosphorus (AP)

255   was determined using the molybdenum blue colorimetric method after extraction with 0.5 M

256   sodium bicarbonate (Bao 2000). The soil redox potential depolarization automatic tester (FJA-

257   6, Chuan-Di Instrument & Equipment Ltd., Nanjing, China) was used to determine *in situ*

258   oxidation-reduction potential (ORP). The porewater pH value was measured *in situ* using a

259   portable pH meter (pHS-25, Leici Instrument Ltd., Shanghai, China). 10 g of soil samples were

260   mixed with 5 volumes of water and extracted leach liquor from the mixture to measure the

261   content of major ions, including SO_4^{2-}, CO_3^{2-}, HCO_3^-, K^+, and Mg^{2+}. The content of SO_4^{2-}, K^+,

262   and Mg^{2+} were measured using a Dionex ICS- 2000 ion chromatograph (Dionex Corporation,

263   Sunnyvale, CA, USA), and CO_3^{2-} and HCO_3^- were determined based on the method of dual

264   indicator-neutralization titration (Bao 2000). The soil microbial biomass carbon (MBC) and

265   microbial biomass nitrogen (MBN) were determined by fumigation extraction method (Vance

266 et al. 1987), using an elemental analyzer (Elementar Vario EL III CHNOS, Elementar

267 Analysensysteme GmbH, Langenselbold, Germany).

268

269 *Data analysis*

270 The differences in measured variables between the waterlogging and non-waterlogging

271 conditions (within the same salinity level) were tested using an independent-samples t-test, and

272 the differences in measured variables among the salinity levels (within the same water level)

273 were tested using one-way ANOVA (analysis of variance). All the data groups met the

274 assumptions of normality based on the Kolmogorov-Smirnov test. The main effects of

275 waterlogging and salinity treatments and their interactive effects on the soil physicochemical

276 variables, plant biomass, $\delta^{13}C$, net ^{13}C-assimilate, percentage of ^{13}C allocation in leaves, stems,

277 and roots, root:shoot ratio, and $\delta^{13}C$ in rhizosphere soil were tested via two-way ANOVA with

278 Tukey's test of multiple comparisons. Statistical analyses were performed using SPSS (version

279 19.0, IBM Inc., USA). Significance was determined at $P < 0.05$.

280 Redundancy analysis (RDA) was further used to test the multiple effects of environmental

281 factors (water level, salinity, and their interactions) and edaphic factors (except for MBC and

282 MBN) on the percentage of ^{13}C allocated in plant organs and soils (Legendre and Legendre

283 1998). RDA was performed with CANOCO 4.5 (Microcomputer Power, Ithaca, NY, USA). A

284 linear regression model was further used to describe the relationships between the MBC and

285 MBN and $\delta^{13}C$ in soils.

286

287

288   **RESULTS**

289   *Allometric biomass growth*

290   Over the experimental period from Day 0 to 150 leaf and stem biomass sharply increased,

291   peaked at Day 96, followed by a decline, while root biomass continued to increase until Day

292   150 (Fig. 1). At the end of the growing season (Day 150), irrespective of saline treatments,

293   waterlogging treatments decreased the leaf, stem, and root biomass by 1.9 to 3.4% on average

294   compared to non-waterlogging conditions. Regardless of the water level, a slight salinity

295   elevation (5 ppt) increased the leaf, stem, and root biomass by 14.6, 2.1, and 14.5%, respectively,

296   compared to non-saline treatments. However, high salinity (15 and 30 ppt) significantly ($P <$

297   0.05) decreased plant biomass growth by 42.5 to 73.1% for leaf biomass, 42.1 to 76.0% for

298   stem biomass, and 8.5 to 36.3% for root biomass compared to non-saline treatments. The

299   combined treatments of waterlogging and high salinity (15 and 30 ppt) resulted in the lowest

300   biomass in leaf, stem, and root tissues. The main effects of salinity on plant biomass growth

301   were significant ($P < 0.05$). The interactive effects of waterlogging × salinity on the leaf and

302   root biomass were significant ($P < 0.01$) (Table S1).

303

304   *^{13}C composition in plant tissues and rhizosphere soil*

305   The $\delta^{13}C$ values in leaves of *P. australis* were highest immediately after the marking at Day 0

306   (5 hours after labeling) and then declined over time (Fig. 2). The $\delta^{13}C$ values in the stems and

307   roots maintained at a high level during the early stage after marking while the values declined

308   during the middle (Day 96) and later (Day 150) growing periods. The $\delta^{13}C$ values in the

309   rhizosphere soil increased rapidly to a peak at Day 1, whereafter and then the values decreased

310 steadily until nearly reaching the natural abundance at Day 150.

311 After labeling and during the early stage (Day 0 to 3), regardless of salinity levels, the δ^{13}C

312 values decreased in leaves, stems, and roots in the waterlogging treatments by on average 7.4

313 to 21.2%, whereas it increased in the soil by 0.3% compared to the non-waterlogging treatments

314 (Fig. 2). Irrespective of water levels, at a salinity of 5 ppt the δ^{13}C values decreased in leaves,

315 stems, and soils by on average 29.4% ($P < 0.05$), 22.2%, and 4.2%, respectively, while δ^{13}C in

316 the roots increased by 45.2% ($P < 0.05$) compared to the non-saline treatment. At high salinity

317 (15 and 30 ppt), the δ^{13}C values significantly decreased in plant organs and soils by on average

318 20.2 to 78.5% (Fig. 2). The combined treatments of waterlogging and high salinity (15 and 30

319 ppt) resulted in the lowest δ^{13}C in leaf, stem, and root tissues and soils. The main effects of

320 waterlogging and salinity on leaf δ^{13}C content in leaves, stems, roots, and soils were significant

321 ($P < 0.05$) (Table S1). No significant interaction occurred between waterlogging and salinity.

322 Later during the growing season (Day 96 to 150), regardless of salinity levels, the δ^{13}C

323 values in leaves, stems, roots, and soils in the waterlogging treatments with a significant

324 decrease for stems by 174% ($P < 0.05$, Fig. 2). Irrespective of water levels, the elevated salinity

325 treatment significantly ($P < 0.05$) reduced the δ^{13}C values in all plant organs by 18.5 to 158.3%

326 and in soils by 1.1 to 4.1%. The lowest δ^{13}C was observed under combined treatments of

327 waterlogging and salinity (15 and 30 ppt) in stem and root tissues and soils. The main effects

328 of the waterlogging and salinity on the δ^{13}C values in all plant organs and soils were significant

329 ($P < 0.05$), except for the effects of waterlogging on root δ^{13}C. The interactive effects between

330 waterlogging and salinity on the δ^{13}C values in leaves, roots, and soils were significant ($P <$

331 0.05) (Table S1).

332

Net ^{13}C allocation in plant organs

From measuring rates of ^{13}C fixation in plant organs (Fig. S1), the allocation of photosynthetic

C within plants was assessed (Fig. 3). Initially after labeling, most ^{13}C accumulated in the leaves.

During the growing season, an increasing amount of ^{13}C was allocated to stems and roots. Until

the end of the growing season (Day 150), the highest percentages of ^{13}C were observed in the

roots.

During the early growing stage, regardless of salinity levels, waterlogging treatments

decreased $^{13}C_L$% by 8.1% and increased $^{13}C_S$% and $^{13}C_R$% by 3.4% and 29.3%, respectively

(Fig. 3), compared to non-waterlogging conditions. Irrespective of water levels, elevating the

salinity to 5 ppt salinity decreased $^{13}C_L$% by on average 11.6% while it increased $^{13}C_S$% and

$^{13}C_R$% by on average 1.9 and 81.7% ($P < 0.05$), respectively, compared to the non-saline groups.

High salinity treatments (15 and 30 ppt) decreased $^{13}C_L$% and $^{13}C_S$% by 8.3 to 16.3% and 7.8

to 11.1%, respectively, while it significantly increased $^{13}C_R$% by 103.4 to 152.5% ($P < 0.05$).

The main effects of waterlogging and salinity on $^{13}C_L$% were significant ($P < 0.05$). There were

no significant interactive effects of waterlogging × salinity (Table S1).

Later during the growing season, regardless of salinity levels, waterlogging treatments

increased $^{13}C_L$% and $^{13}C_R$% by on average 5.7 and 26.8% ($P < 0.05$), respectively, while they

decreased $^{13}C_S$% by 30.5% ($P < 0.05$) compared to non-waterlogging treatments (Fig. 3).

Irrespective of water levels, elevating the salinity to 5 ppt salinity significantly ($P < 0.05$)

decreased $^{13}C_L$% and $^{13}C_S$% by on average 48.4% and 39.0%, respectively, while it significantly

($P < 0.05$) increased $^{13}C_R$% by on average 50.7% compared to the non-saline groups. The 15

354   ppt salinity decreased $^{13}C_L$% and $^{13}C_S$% by on average 37.9% ($P < 0.05$) and 2.0%, respectively,

355   while it increased $^{13}C_R$% by 6.7% on average. Thirty ppt salinity significantly ($P < 0.05$)

356   decreased $^{13}C_L$% and $^{13}C_S$% by on average 28.7% and 55.8%, respectively, while it significantly

357   ($P < 0.05$) increased $^{13}C_R$% by on average 67.9%. The combined treatments of waterlogging

358   and high salinity (30 ppt) resulted in the lowest $^{13}C_S$% and the highest $^{13}C_R$%. The main effects

359   of waterlogging and salinity on $^{13}C_S$% and $^{13}C_R$% were significant ($P < 0.05$). The interactive

360   effects of waterlogging × salinity on $^{13}C_L$% were significant ($P < 0.05$) (Table S1).

361

Soil physicochemical variables

363   Regardless of salinity levels, waterlogging treatment significantly ($P < 0.05$) decreased the AN,

364   AP, ORP, K^+, MBC and MBN by on average 12.0 to 52.0% and decreased the pH and Mg^{2+} by

365   on average 0.6 to 22.9%, while HCO_3^- and SO_4^{2-} increased by on average 5.5 to 66.9% ($P <$

366   0.05), respectively, compared to non-waterlogging conditions (Fig. 4). Regardless of the water

367   table, increasing salinity decreased almost all the soil variables compared to 0 ppt conditions,

368   except for the concentrations of HCO_3^-, SO_4^{2-} and K^+ (Fig. 4). The lowest AN, AP, ORP, pH,

369   Mg^{2+}, MBC and MBN and the highest HCO_3^- and SO_4^{2-} were observed under the combined

370   treatments of waterlogging and high salinity (30 ppt). The main effects of waterlogging and

371   salinity treatments on the edaphic factors were significant ($P < 0.05$), except for pH, HCO_3^-,

372   and AP (Table 1). The interactive effects of waterlogging × salinity on HCO_3^-, K^+, Mg^{2+}, and

373   MBN were significant ($P < 0.05$).

374

Effects of environmental factors on ^{13}C character

376   Redundancy analysis (RDA) revealed that the first two principal components explained 73.4%

377   and 52.4% of the total variation in the treatment-induced changes in the plant–soil ^{13}C allocation

378   during the early (Fig. 5a) and later growing periods (Fig. 5b), respectively. The increased

379   salinity made a stronger contribution to the relative influence on C allocation patterns than that

380   of water-level treatments during the early growing stage while it showed the opposite during

381   the later growing season (Table 2). At the early stage, the contribution of the combined

382   treatments of waterlogging × salinity on the C allocation pattern was lower than that of the

383   single salinity treatments while it was higher (37.6%) than the contribution of the single salinity

384   treatments (22.3%) during the later growing season (Table 2).

385

386

387   **DISCUSSION**

388   *Temporal variation in C allocation patterns*

389   Plants mainly use three ways to allocate newly fixed C, including incorporation into plant

390   shoots as structural components, release of CO_2 into the atmosphere due to respiration, and

391   transfer of C to below-ground roots resulting in increased soil organic matter content. ^{13}C pulse

392   labeling offers a method to track recently fixed photosynthetic assimilates from aboveground

393   and belowground plant parts and soils (e.g., Kuzyakov and Gavrichkova 2010; Ge et al. 2012).

394   After the initial labeling, most ^{13}C was measured in aboveground plant parts. Subsequently, we

395   detected a consistent increase in δ^{13}C from Day 0 to Day 3 in plant roots. This aligned with

396   results by Johnson et al. (2002) and Ostle et al. (2000), showing a significant ^{13}C enrichment in

397   roots within 4 hours of the labeling that peaked between 24 and 48 hours after the treatment.

This demonstrated a potential importance of recently fixed C for metabolic activity. Results that were supported by Lu et al. (2002a), who found that most photosynthetic C was retained in the aboveground plant parts soon after treatments while a smaller fraction of the assimilated C was transferred to belowground organs.

In our mesocosm experiments, only the rhizosphere soil was sampled to trace the ^{13}C flow from plant to soil, as the rhizosphere soil contained more enriched ^{13}C compared to deeper soil layers (data not presented). We found that the rhizosphere soil $\delta^{13}C$ increased to a peak value during Day 1, suggesting a fast transport of the fixed C from plants into the soil via rhizodeposition. Rhizodeposition is composed of a range of exudates, secretions, and dead cells sloughed from root caps and senescing roots (Leak et al. 2006). This short-term increase in soil $\delta^{13}C$ supported that the release of recent photosynthetic C into soils via root exudation occurs within 1–2 days after labeling, in agreement with Murray et al (2004). The released root-derived C has been shown to consist mainly of easily mineralizable components (Lu et al. 2002b), which are further released as $^{13}C\text{-}CO_2$ via microbial respiration (Kuzyakov and Gavrichkova 2010), a process that leads to a rapid depletion of ^{13}C in soil. In addition, we observed that the soil $\delta^{13}C$ decreased from Day 1 after labeling. Hereafter, we anticipated a fraction of the ^{13}C to be transformed to stable C stored in the soil pool following the processes suggested by Kaštovská and Šantrůčková (2007). At the end of the growing season (Day 150), an excessive ^{13}C signal could still be detected against the natural abundance, which supports previous findings that a portion of the structural C components in plants generated from photosynthates is released into the soil as decaying root tissues and detritus with progression of the growing season (Lu et al. 2002a).

420

Effects of prolonged waterlogging

Our results showed that waterlogging treatments alone did not affect C allocation in leaves and stems but did significantly increase C allocation to roots during the later growth period. Waterlogging conditions often produce anaerobic environments with lower ORP and following accumulation of toxic compounds in soils, with detrimental effects to plant growth (DeLaune et al. 1987). Poorter et al. (2012) reported that plants allocate relatively more biomass to roots if the limiting factor for growth is belowground (e.g., inundation or nutrient deficit). The "optimal partitioning theory" (Gedroc et al. 1996) states that plants preferentially allocate biomass and nonstructural carbohydrates to acquire the resource that most limits growth (Kobe et al. 2010). As observed in this study, the root:shoot ratio increased under waterlogging conditions (0.65±0.32 *vs.* 0.56±0.25) relative to non-waterlogging conditions (Fig. 1). Minden et al. (2012) reported that marsh plants growing in sandy areas with high inundation allocated more biomass to roots and rhizomes than to above-ground growth. Pezeshki et al. (1997) also reported that a coastal mangrove seedling (*Rhizophora mangle*) under low soil redox conditions (or increased inundation) showed an apparent shift in biomass allocation favoring root C allocation.

Extensive development of aerenchyma under waterlogging conditions can also to some extent contribute to higher percentage of ^{13}C allocation in roots. Armstrong et al. (1999) indicated that the roots of submerged *P. australis* tended to develop more extensive aerenchyma than those of controls whose shoots were emergent. The allocation of photosynthetic carbon in the below-ground parts can also be affected by soil physical and chemical properties (Wang et

442   al. 2019b). Our results showed that waterlogging treatments had significant effects mainly on

443   the SO_4^{2-} concentration in the soil (Table S1), which had the second largest relative contribution

444   (Table S3) to the allocation patterns among the edaphic factors. Furthermore, the percentage of

445   ^{13}C allocated to roots was positively related to the SO_4^{2-} concentration (Fig. S3). We also found

446   that waterlogging treatments significantly decreased the soil nutrients (i.e., AN and AP)

447   compared to non-waterlogging conditions. Soil nutrient shortages are prone to further increase

448   the proportion of plant photosynthates to roots in wetland vegetation (Cronin and Lodge 2003).

449   Based on previous studies, the C allocation pattern within plants of different coastal

450   species is not consistent as a result to stress treatments (Van Bodegom et al. 2008; Gao et al.

451   2015; Martínez-Alcántara et al. 2012; Xue et al. 2018). Naidoo and Naidoo (1992) reported a

452   converse allocation pattern, showing that increased flooding shifted resource allocation from

453   belowground components to aerial organs of a coastal wetland grass, *Sporobolus virginicus*. In

454   addition, Xue et al. (2018) reported that the marsh species *Scirpus mariqueter* and *Spartina*

455   *alterniflora* had a neutral response of its biomass allocation from increasing flooding depth. It

456   cannot be ruled out however, that this could be due to different methods of hydrological

457   treatments including persistent waterlogging and intermittent flooding as well as the difference

458   in species. Another possible explanation is that the root:shoot ratio data available might not be

459   sufficient to conclude on the C allocation changes.

460   The $^{13}CO_2$ source–sink relationship within the *P. australis* plant–soil system might add to

461   the complexity of the ^{13}C allocation patterns and complicate identification of simple causation.

462   The $^{13}CO_2$ source–sink relationship consists of the allocation rates of photosynthetic $^{13}CO_2$,

463   shoot $^{13}CO_2$ respiration, and soil $^{13}CO_2$ emissions. In the current study, waterlogging treatments

464 did not significantly affect the photosynthesis rates ($F = 0.865$, $P = 0.354$, Fig. S2) or shoot ^{13}C

465 respiration ($F = 0.021$, $P = 0.886$) (Fig. S2). Thus, the severely inhibited soil $^{13}CO_2$ respiration

466 under waterlogging conditions may partially account for the increased C allocation to plant

467 roots. Previous studies found severely decreased root respiration (*S. alterniflora*, Dai and

468 Wiegert 1996) and soil CO_2 efflux (alpine wetlands, Gao et al. 2015) under waterlogging

469 conditions. Although the ^{13}C accumulation in rhizosphere soil was higher at the beginning of

470 the labeling period (Day 0 and Day 1), the remaining ^{13}C assimilation recovered in the soils

471 displayed a great decline during the middle and later growing season (Fig. 2), moreover, the

472 ^{13}C under waterlogging condition was lower than that under non-waterlogging condition. This

473 was consistent with Tian et al. (2013), who stated that the ^{14}C recovery in flooded paddy soil

474 was lower than that in non-flooded soils (5.3% *vs.* 10.8%) at 45 days after labeling. They

475 explained this due to lower ^{14}C exudation from roots into the soil. The amount of ^{13}C deposited

476 in the soils was mainly driven by root biomass growth; therefore, the inhibited root biomass

477 under waterlogging conditions would to some extent account for the decreased ^{13}C recovered

478 in the soil (Kotas et al. 2019). Another cause might be that excessive soil moisture has shown

479 to accelerate carbon turnover from rhizosphere soil to other carbon pools.

480

481 ***Effects of elevated salinity***

482 In this study, elevated salinity led to significantly increased allocation percentage ^{13}C in roots

483 compared to non-saline groups (0 ppt) over the growing season (Fig. 5). The increased C

484 allocation into roots was in agreement with previous studies demonstrating an increased

485 root:shoot ratio of *P. australis* with increased salinity (Lissner et al., 1999; Scarton et al. 2002;

Xue et al. 2018). Previous studies in *S. nipponicus* marshes and mangrove wetlands have showed an increased root:shoot ratio with elevated salinity (Ball, 1988; Tang et al. 2021). Excessive salinity may hinder the normal metabolism of plants via osmotic stress and ion poisoning and hamper plant photosynthesis by limiting synthesis of chlorophyll, gas exchange, and stomatal conductance (DeLaune et al. 1987; Pagter et al. 2009; Li et al. 2018). NaCl toxicity will directly hinder carbon translocation in the phloem (Suwa et al. 2006, 2008). Inhibited photosynthetic net C assimilation alters the C allocation pattern within plant pools (Soetaert et al. 2004; Ge et al. 2012; Wang et al. 2019b). For instance, Soetaert et al. (2004) compared two reed marshes with different salinities (oligohaline *vs.* mesohaline marsh) and found that a higher proportion of assimilates were transported back toward the rhizome-root system at the mesohaline site than at the oligohaline site (54% *vs.* 45%). Reeds in mesohaline environments were constrained to invest more energy to maintain the metabolic integrity of the plant. Pérez-López et al. (2014) suggested increased carbohydrate partitioning to the belowground organs under stress conditions, showing a higher natural $\delta^{13}C$ value in the roots than in leaves. A likely reason for this is that the roots were the first organs to face salt stress and to maintain water and mineral uptake. As such, the effect of elevated salinity on plant C allocation patterns is consistent with the 'optimal partitioning' theory (Kobe et al. 2010).

Here we found that HCO_3^- and SO_4^{2-} ions and nutrients had a high relative contribution to the C allocation patterns among the edaphic factors (Table S3). The concentrations of HCO_3^- and SO_4^{2-} in soil were positively related to the percentage of ^{13}C allocated to roots, while AN had negative effects (Fig. S3). This demonstrated that increased HCO_3^- and SO_4^{2-} ions and nitrogen shortage induced by elevated salinity could contribute to a larger ^{13}C allocation into

508   plant roots. In context, Rietz and Haynes (2003) reported that organic matter decomposition

509   was inhibited by increasing salinity which might cause a substantial decline in potentially

510   available N, while Xie et al. (2020) observed that the total microbial biomass of marsh soils

511   was adversely affected by soil salinity. Furthermore, Bai et al. (2012) reported that the amount

512   of available N generally showed a negative relationship with soil salinity.

513   Although the C allocation rates towards roots were higher under elevated salinity than

514   under non-saline conditions, the total amount of photosynthate and ^{13}C recovered in both

515   aboveground and belowground parts decreased under high salinity in our studies. This could be

516   ascribed to the decrease in net C assimilation of *P. australis* as a response to elevated salinity

517   (Li et al. 2020). Furthermore, the ^{13}C accumulation in rhizosphere soil decreased with

518   increasing salinity over the growing season probably due to decreased root exudates or root-

519   deprived materials (Fig. 2). This observation matches those by Li et al. (2016), reporting that

520   the soil organic ^{13}C content in a high-salinity marsh was significantly lower than that in a low-

521   salinity marsh 90 days after $^{13}CO_2$ labeling. Likewise, Xue et al. (2020) showed a significantly

522   negative correlation between soil salinity and soil organic matter in a manipulated pot

523   experiment with marsh soils. High salinity in coastal wetlands could also restrain soil microbial

524   activities and organic C accumulation (Zhao et al. 2017), therefore, the significantly positive

525   relationships between MBC, MBN and δ^{13}C in *P. australis* soil might partially explain the

526   effects of waterlogging and salinity on rhizosphere soil δ^{13}C (Fig. S4). In addition, high salinity

527   can destabilize soil organic matter in marsh wetlands (Williams and Rosenheim 2015); as a

528   result, the ^{13}C previously incorporated into soil organic matter would become liable and

529   remineralized, leading to less remaining ^{13}C in the soil. In conclusion, although elevated salinity

530   in coastal marshes promoted C transport to plant organs belowground the net C contribution to

531   the soil C pool might decline.

532   In this study, we used NaCl solutions to simulate saline environments in the plant-soil

533   mesocosms. However, other ions in sea water such as potassium and sulfate may also affect the

534   soil microbial community and enzymatic activity (Chambers et al. 2013, 2016), likely

535   influencing plant growth and carbon allocation in plants and soils. Due to the multi-factor

536   effects of seawater intrusion, the parallel experiment with artificial seawater instead of only

537   NaCl solution is still needed.

538

539   ***Effects of combined waterlogging and elevated salinity***

540   Based on the RDA results from the initial phase of the experimental treatments, the combined

541   effects of waterlogging and elevated salinity did not contribute additionally to the C allocation

542   patterns in plant organs and rhizosphere soils than during elevated salinity only (33.4% *vs.*

543   65.7%, Table 2). Hereafter, during the middle of the growing season waterlogging showed to

544   enhance the effects of salinity treatments on the C allocation patterns. Towards the end of the

545   growing season (Day 150), inhibition of growth in both above- and belowground plant parts

546   limited the net ^{13}C assimilation and consequently the net ^{13}C transportation into roots, leading

547   to the lowest remaining ^{13}C in roots measured under combined waterlogging and high salinity.

548   The RDA results showed that the combined hydrological treatments had a higher relative

549   contribution to the C allocation patterns compared to the salinity only treatment (37.6% for

550   waterlogging × salinity *vs.* 22.3% for salinity). These observations correspond to previous

551   studies having shown that the combined stresses of waterlogging and salinity can hinder

552   adventitious root formation in coastal vegetation (Spalding and Hester 2007) or impair root

553   function by increasing the concentrations of Na^+ and Cl^- in plant organs (Barrett-Lennard 2003).

554   As a result, the limited root growth might affect the aboveground organs due to abnormal

555   physiological functions (DeLaune et al. 1993).

556   Overall, the remaining ^{13}C in roots is mainly determined by C transportation from

557   aboveground parts and exportation from the roots into soils (through exudation) and root

558   respiration (Tian et al. 2013). Root exudation might be inhibited by waterlogging and salinity.

559   On the other hand, root respiration of coastal plants can be suppressed by both waterlogging

560   and salinity (Burchett et al. 1989; Krauss et al. 2012). The decline in both root exudation and

561   respiration can be conducive to ^{13}C accumulation in roots. Furthermore, the ^{13}C allocation

562   percentage in roots showed the highest value under combined treatments of waterlogging and

563   high salinity. This indicated an adaptive mechanism of *P. australis* to transport more C to

564   belowground when exposed to harsh environmental stress (Soetaert et al. 2004). In addition,

565   the severely suppressed N availability under combined waterlogging and high salinity (Fig. 4a)

566   would also facilitate ^{13}C allocation into roots (Cronin and Lodge 2003).

567   The combination of waterlogging and salinity had no significant effects on rhizosphere

568   soil $\delta^{13}C$ during the early labeling phase (Table S1). After the initial labeling, the released root-

569   derived C mainly consists of easily mineralizable components, and most of the products might

570   be transformed into MBC in soil and CO_2 release of respiration (Lu et al. 2002b; Marx et al.

571   2010). In addition, a portion of the additional ^{13}C will likely enter the soil pool via

572   rhizodeposition or dead litter. At the end of the growing season, the lowest MBC and MBN

573   were observed under the combined treatments of waterlogging and high salinity. The combined

574   hydrological treatments significantly affected soil $\delta^{13}C$, which might be ascribed to the

575   amplifying effect of waterlogging and salinity over a longer time period. During the growth

576   season, the remaining soil ^{13}C is involved in many biochemical processes, such as C emission

577   by root respiration, transformation into water-extractable organic C, resistant C in soil, and C

578   utilization by microorganisms (Marx et al. 2010). In view of the complex soil C processes, more

579   work is needed to distinguish the various C forms and their fates in the plant-soil system under

580   changing hydrological conditions in coastal marshes.

581

582

583   **CONCLUSIONS**

584   By employing the $^{13}CO_2$ pulse-labeling approach we explored the impacts of sea level rise

585   (waterlogging and salinity elevation) on the accumulation and allocation of photosynthetic C

586   within the *P. australis* plant-soil systems. Overall, the results demonstrate that waterlogging

587   and elevated salinity treatments decreased the photosynthetic C accumulation in plants.

588   Treatments with both waterlogging and elevated salinity reduced the ^{13}C transport to the organs

589   of *P. australis* and significantly increased the ^{13}C allocation percentage to belowground tissue,

590   indicating an acclimation strategy of *P. australis* under environmental stresses. The changed

591   hydrology showed no significant effect on ^{13}C recovered in rhizosphere soils, while high

592   salinity treatments significantly reduced ^{13}C recovered in soils, suggesting a decrease in C

593   exudation from roots in saline environments. Waterlogging enhanced the effects of salinity on

594   the ^{13}C allocation pattern, particularly during the late growing season. The responses of C

595   allocation in plant organs and rhizosphere soils to the hydrological treatments can be related to

596 changes in nutrient, ionic concentrations and soil microbial biomass. In conclusion, the

597 expected SLR projection with prolonged flooding and saltwater intrusion into marsh lands

598 might decrease total C stocks and alter the C allocation pattern in marsh plant-soil systems.

599

ACKNOWLEDGMENT

Conflict of interest

The authors declare that they have no conflict of interest.

REFERENCES

Alongi, DM (2012) Carbon sequestration in mangrove forests. Carbon Manag 3: 313-322

Armstrong J, Afreen-Zobayed F, Blyth S, Armstrong W (1999) *Phragmites australis*: effects of shoot submergence on seedling growth and survival and radial oxygen loss from roots. Aquat Bot 64:275-289

Bai J, Gao H, Xiao R, Wang J, Huang C (2012) A review of soil nitrogen mineralization as affected by water and salt in coastal wetlands: issues and methods. Clean - Soil Air Water

40:1099-1105

Ball MC (1988) Salinity tolerance in the mangroves *Aegiceras corniculatum* and *Avicennia marina*. I. Water use in relation to growth, carbon partitioning, and salt balance. Funct Plant Biol 15:447-464

Bao SD (2000) Methods of Soil Agro-chemistry Analysis. Beijing, China (in Chinese)

Barrett-Lennard EG 2003 The interaction between waterlogging and salinity in higher plants: causes, consequences and implications. Plant Soil 253:35-54

Burchett MD, Clarke CJ, Field CD, Pulkownik A (1989) Growth and respiration in two mangrove species at a range of salinities. Physiol Plantarum 75:299-303

Cronin G, Lodge DM (2003) Effects of light and nutrient availability on the growth, allocation, carbon/nitrogen balance, phenolic chemistry, and resistance to herbivory of two freshwater macrophytes. Oecologia 137:32-41

Chambers LG, Guevara R, Boyer JN, Troxler TG, Davis SE (2016) Effects of salinity and inundation on microbial community structure and function in a mangrove peat soil. Wetlands 36:361–371

Chambers LG, Osborne TZ, Reddy KR (2013) Effect of salinity-altering pulsing events on soil organic carbon loss along an intertidal wetland gradient: a laboratory experiment. Biogeochemistry 115:363–383

Dai T, Wiegert RG (1996) Estimation of the primary productivity of *Spartina alterniflora* using a canopy model. Ecography 19:410-423

DeLaune RD, Pezeshki SR, Patrick Jr WH (1987) Response of coastal plants to increase in submergence and salinity. J Coast Res 535-546

DeLaune RD, Pezeshki SR, Patrick WH (1993) Response of coastal vegetation to flooding and salinity: a case study in the rapidly subsiding Mississippi River deltaic plain, USA. In: Interacting stresses on plants in a changing climate. Springer, Berlin, Heidelberg, pp 211-229

Gao JQ, Gao JJ, Zhang XW, Xu XL, Deng ZH, Yu FH (2015) Effects of waterlogging on carbon assimilate partitioning in the Zoige alpine wetlands revealed by $^{13}CO_2$ pulse labeling. Sci Rep 5:1-5

Ge ZM, Wang TH, Wang KY, Wang, XM (2008) Characteristics of coastal wetland ecosystem of the Yangtze Estuary and conservation for key communities. Science Press, Beijing, China, pp. 28-29 (in Chinese)

Ge ZM, Zhou X, Kellomäki S, Biasi C, Wang KY, Peltola H, Martikainen PJ (2012) Carbon assimilation and allocation (^{13}C labeling) in a boreal perennial grass (*Phalaris arundinacea*) subjected to elevated temperature and CO_2 through a growing season. Environ Exp Bot 75:150-158

Gedroc JJ, McConnaughay KDM, Coleman JS (1996) Plasticity in root/shoot partitioning: optimal, ontogenetic, or both? Funct Ecol 10:44-50

Hoagland DR, Arnon DI (1950) The water-culture method for growing plants without soil. Circ California Agric Exper Station 347:32

IPCC (2019) Summary for Policymakers. In: IPCC Special Report on the Ocean and Cryosphere in a Changing Climate (H.-O. Pörtner, D.C. Roberts, V. Masson-Delmotte, P. Zhai, M. Tignor, E. Poloczanska, K. Mintenbeck, A. Alegría, M. Nicolai, A. Okem, J. Petzold, B. Rama, N.M. Weyer (eds.)]. Cambridge University Press, Cambridge, UK and

New York, NY, USA, pp. 3-35

Johnson D, Leake JR, Ostle N, Ineson P, Read DJ (2002) In situ $^{13}CO_2$ pulse-labeling of upland grassland demonstrates a rapid pathway of carbon flux from arbuscular mycorrhizal mycelia to the soil. New Phytol 153:327-334

Kaštovská E, Šantrůčková H (2007) Fate and dynamics of recently fixed C in pasture plant–soil system under field conditions. Plant Soil 300:61-69

Kirwan ML, Mudd SM (2012) Response of salt-marsh carbon accumulation to climate change. Nature 489:550-553

Kobe RK, Iyer M, Walters MB (2010) Optimal partitioning theory revisited: nonstructural carbohydrates dominate root mass responses to nitrogen. Ecology 91:166-179

Kotas P, Edwards K, Jandová K, Kaštovská E (2019) Interaction of fertilization and soil water status determine C partitioning in a sedge wetland. Soil Biol Biochem, 135:85-94

Krauss KW, Whitbeck JL, Howard RJ (2012) On the relative roles of hydrology, salinity, temperature, and root productivity in controlling soil respiration from coastal swamps (freshwater). Plant Soil 358:265-274

Kutzbach L, Wagner D, Pfeiffer EM (2004) Effect of microrelief and vegetation on methane emission from wet polygonal tundra, Lena Delta, Northern Siberia. Biogeochemistry 69:341-362

Kuzyakov Y, Gavrichkova O (2010) Time lag between photosynthesis and carbon dioxide efflux from soil: a review of mechanisms and controls. Global Change Biol 16:3386-3406.

Leake JR, Ostle NJ, Rangel-Castro JI, Johnson D (2006) Carbon fluxes from plants through soil organisms determined by field $^{13}CO_2$ pulse-labeling in an upland grassland. Appl Soil

Ecol 33:152-175

Legendre P, Legendre L (1998) Numerical Ecology. Elsevier Amsterdam, New York

Li L, Qiu S, Chen Y, Xu X, Zhao X, Christie P, Xu M (2016) Allocation of photosthestically-fixed carbon in plant and soil during growth of reed (*Phragmites australis*) in two saline soils. Plant Soil 404:277-291

Li SH, Ge ZM, Xie LN, Chen W, Yuan L, Wang DQ, Li XZ, Zhang LQ (2018) Ecophysiological response of native and exotic salt marsh vegetation to waterlogging and salinity: Implications for the effects of sea-level rise. Sci Rep 8:1-13

Li YL, Ge ZM, Xie LN, Li SH, Tan LS (2022) Effects of waterlogging and salinity increase on CO2 efflux in soil from coastal marshes. Appl Soil Ecol 170:104268

Li YL, Guo HQ, Ge ZM, Wang DQ, Liu WL, Xie LN, Li SH, Tan LS, Zhao B, Li XZ, Tang JW (2020) Sea-level rise will reduce net CO_2 uptake in subtropical coastal marshes. Sci Total Environ 747:141214

Lissner J, Schierup HH, Comín FA, Astorga V (1999) Effect of climate on the salt tolerance of two *Phragmites australis* populations.: I. Growth, inorganic solutes, nitrogen relations and osmoregulation. Aquat Bot 64:317-333

Lu Y, Watanabe A, Kimura M (2002a) Input and distribution of photosynthesized carbon in a flooded rice soil. Global Biogeochem Cy 16:32-1

Lu Y, Watanabe A, Kimura M (2002b) Contribution of plant-derived carbon to soil microbial biomass dynamics in a paddy rice microcosm. Biol Fertil Soils 36:136-142

Luo Y, Sherry R, Zhou X, Wan S (2009) Terrestrial carbon-cycle feedback to climate warming: experimental evidence on plant regulation and impacts of biofuel feedstock harvest. Gcb

Bioenergy 1:62-74

Martínez-Alcántara B, Jover S, Quiñones A, Forner-Giner MÁ, Rodríguez-Gamir J, Legaz F, Primo-Millo E, Iglesias DJ (2012) Flooding affects uptake and distribution of carbon and nitrogen in citrus seedlings. J Plant Physiol 169:1150-1157

Marx M, Buegger F, Gattinger A, Zsolnay Á, Charles Munch J (2010) Determination of the fate of regularly applied ^{13}C-labeled-artificial-exudates C in two agricultural soils. Soil Sci Plant Nutr 173:80-87

Mauchamp A, Méthy M (2004) Submergence-induced damage of photosynthetic apparatus in Phragmites australis. Environ Exp Bot 51:227-235

Mcleodr E, Chmura GL, Bouillon S, Salm R, Björk M, Duarte CM, Lovelock CE, Schlesinger WH, Silliman BR (2011) A blueprint for blue carbon: toward an improved understanding of the role of vegetated coastal habitats in sequestering CO_2. Front Ecol Environ 9:552-560

Minden V, Andratschke S, Spalke J, Timmermann H, Kleyer M (2012) Plant trait–environment relationships in salt marshes: Deviations from predictions by ecological concepts. Perspect Plant Ecol 14:183-192

Moodley L, Boschker HTS, Middelburg JJ, Pel R, Herman PMJ, De Deckere E, Heip CHR (2000) Ecological significance of benthic foraminifera: ^{13}C labeling experiments. Mar Ecol Prog Ser 202:289-295

Murray P, Ostle N, Kenny C, Grant H (2004) Effect of defoliation on patterns of carbon exudation from *Agrostis capillaris*. Soil Sci Plant Nutr 167:487-493

Naidoo G, Naidoo S (1992) Waterlogging responses of *Sporobolus virginicus* (L.) Kunth.

Oecologia 90:445-450

Neubauer SC, Franklin RB, Berrier DJ (2013) Saltwater intrusion into tidal freshwater marshes alters the biogeochemical processing of organic carbon. Biogeosciences 10:8171-8183

Ostle N, Ineson P, Benham D, Sleep D (2000) Carbon assimilation and turnover in grassland vegetation using an in situ $^{13}CO_2$ pulse labeling system. Rapid Commun Mass Spectrom 14:1345-1350

Pagter M, Bragato C, Malagoli M, Brix H (2009) Osmotic and ionic effects of NaCl and Na_2SO_4 salinity on *Phragmites australis*. Aquat Bot 90:43-51

Pérez-López U, Mena-Petite A, Muñoz-Rueda A (2014) Will carbon isotope discrimination be useful as a tool for analysing the functional response of barley plants to salinity under the future atmospheric CO_2 conditions?. Plant Sci 226:71-81

Pezeshki SR, DeLaune RD (1997) Population differentiation in *Spartina patens*: Responses of photosynthesis and biomass partitioning to elevated salinity. Bot Bull Acad Sin 38

Pezeshki SR, DeLaune RD, Meeder JF (1997) Carbon assimilation and biomass partitioning in *Avicennia germinans* and *Rhizophora mangle* seedlings in response to soil redox conditions. Environ Exp Bot 37:161-171

Poorter H, Niklas KJ, Reich PB, Oleksyn J, Poot P, Mommer L (2012) Biomass allocation to leaves, stems and roots: meta-analyses of interspecific variation and environmental control. New Phytol 193:30-50

Rietz DN, Haynes RJ (2003) Effects of irrigation-induced salinity and sodicity on soil microbial activity. Soil Biol Biochem 35:845-854

Scarton F, Day JW, Rismondo A (2002) Primary production and decomposition of *Sarcocornia*

fruticosa (L.) Scott and *Phragmites australis* Trin. ex Steudel in the Po Delta, Italy. Estuaries 25:325-336

Simard SW, Perry DA, Jones MD, Myrold DD, Durall DM, Molina R (1997) Net transfer of carbon between ectomycorrhizal tree species in the field. Nature 388:579-582

Soetaert K, Hoffmann M, Meire P, Starink M, van Oevelen D, Van Regenmortel S, Cox T (2004) Modeling growth and carbon allocation in two reed beds (*Phragmites australis*) in the Scheldt estuary. Aquat Bot 79:211-234

Spalding EA, Hester MW (2007) Interactive effects of hydrology and salinity on oligohaline plant species productivity: implications of relative sea-level rise. Estuar Coast 30:214-225

Suwa R, Fujimaki S, Suzui N, Kawachi N, Ishii S, Sakamoto K, Nguyen NT, Saneoka H, Mohapatra PK, Moghaieb RE, Matsuhashi S, Fujita K (2008) Use of positron-emitting tracer imaging system for measuring the effect of salinity on temporal and spatial distribution of ^{11}C tracer and coupling between source and sink organs. Plant Sci 175:210-216

Suwa R, Nguyen NT, Saneoka H, Moghaieb R, Fujita K (2006) Effect of salinity stress on photosynthesis and vegetative sink in tobacco plants. Soil Sci Plant Nutr 52:243-250

Tang H, Bai J, Chen F, Liu Y, Lou Y (2021) Effects of salinity and temperature on tuber sprouting and growth of *Schoenoplectus nipponicus*. Ecosphere 12:e03448

Tian J, Pausch J, Fan M, Li X, Tang Q, Kuzyakov Y (2013) Allocation and dynamics of assimilated carbon in rice-soil system depending on water management. Plant Soil 363:273-285

Titlyanova AA, Romanova IP, Kosykh NP, Mironycheva-Tokareva NP (1999) Pattern and

process in above-ground and below-ground components of grassland ecosystems. J Veg Sci 10:307-320

van Bodegom PM, Sorrell BK, Oosthoek A, Bakker C, Aerts R (2008) Separating the effects of partial submergence and soil oxygen demand on plant physiology. Ecology 89:193-204

Vance ED, Brookes PC, Jenkinson DS (1987) An extraction method for measuring soil microbial biomass C. Soil Biol Biochem 19:703-707

Wang B, Gong J, Zhang Z, Yang B, Liu M, Zhu C, Shi J, Zahng W, Yue K (2019a) Nitrogen addition alters photosynthetic carbon fixation, allocation of photoassimilates, and carbon partitioning of *Leymus chinensis* in a temperate grassland of Inner Mongolia. Agr Forest Meteorol 279:107743

Wang C, Xiao R, Cui Y, Ma Z, Guo Y, Wang Q, Xiu Y, Zhang M (2019b) Photosynthate-13C allocation in the plant-soil system after ^{13}C–pulse labeling of *Phragmites australis* in different salt marshes. Geoderma 347:252-261

Wersal RM, Madsen JD, Cheshier JC (2013) Seasonal biomass and starch allocation of common reed (*Phragmites australis*) (haplotype I) in Southern Alabama, USA. Invasive Plant Sci Manag 6:140-146

Williams EK, Rosenheim BE (2015) What happens to soil organic carbon as coastal marsh ecosystems change in response to increasing salinity? An exploration using ramped pyrolysis. Geochem Geophys 16:2322-2335

Wu Y, Tan H, Deng Y, Wu J, Xu X, Wang Y, Tang Y, Higashi T, Cui X (2010) Partitioning pattern of carbon flux in a *Kobresia* grassland on the Qinghai-Tibetan Plateau revealed by field ^{13}C pulse-labeling. Global Change Biol 16:2322-2333

Xie LN, Ge ZM, Li YL, Li SH, Tan LS, Li XZ (2020) Effects of waterlogging and increased salinity on microbial communities and extracellular enzyme activity in native and exotic marsh vegetation soils. Soil Sci Soc Am J 84:82-98

Xin P, Wilson A, Shen C, Ge Z, Moffett KB, Santos IR, Chen X, Xu X, Yau YYY, Moore W, Li L, Barry DA (2022) Surface water and groundwater interactions in salt marshes and their impact on plant ecology and coastal biogeochemistry. Rev Geophys, 60: e2021RG000740

Xue L, Jiang J, Li X, Yan Z, Zhang Q, Ge Z, Tian B, Craft C (2020) Salinity affects topsoil organic carbon concentrations through regulating vegetation structure and productivity. J Geophys Res-Biogeo 125:e2019JG005217

Xue L, Li X, Yan Z, Zhang Q, Ding W, Huang X, Tian B, Ge Z, Yin Q (2018) Native and non-native halophytes resiliency against sea-level rise and saltwater intrusion. Hydrobiologia 806:47-65

Zhang P, Nie M, Li B, Wu J (2017) The transfer and allocation of newly fixed C by invasive *Spartina alterniflora* and native *Phragmites australis* to soil microbiota. Soil Biol Biochem 113:231-239

Zhao Q, Bai J, Lu Q, Zhang G (2017) Effects of salinity on dynamics of soil carbon in degraded coastal wetlands: implications on wetland restoration. Phys Chem Earth Parts A/B/C 97:12-18

TABLES

Table 1. Main and interactive effects (*F* value) of waterlogging (water) and salinity (salinity) on the edaphic variables.

Variables	Water	Salinity	Water × Salinity
AN	**8.657****	**4.568***	2.088
AP	**26.031****	1.282	1.433
ORP	**150.773****	**4.992***	0.764
pH	2.837	**6.386****	0.368
HCO_3^-	3.291	**20.596****	**4.423***
SO_4^{2-}	**21.168****	**30.703****	1.290
K^+	**42.398****	**52.214****	**6.867****
Mg^{2+}	**6.385***	**4.713***	**3.553***
MBC	**25.239****	**21.077****	2.646
MBN	**120.414****	**34.948****	**5.742****

AN: available nitrogen; AP: available phosphorus; ORP: oxidation-reduction potential; HCO_3^-: bicarbonate ion; SO_4^{2-}: sulfate ion; K^+: potassium ion; Mg^{2+}: magnesium ion; MBC: microbial biomass carbon; MBN: microbial biomass nitrogen.

* significance at $p < 0.05$; ** significance at $p < 0.01$.

Table 2. Explained variance and relative contributions of waterlogging (water) and salinity treatments to the percentage of ^{13}C allocation to leaf, stem, root, and soil $\delta^{13}C$, respectively, during the early and later growth periods. Tests are redundancy analysis (RDA).

Explanatory variable	Dependent variable	Explained variance	Relative contribution	*F*-value	*P*-value
Water		1.0%	1.0%	0.23	0.06
Salinity	Allocation at early stage	69.1%	65.7%	43.14	**<0.01**
Water × Salinity		35.1%	33.4%	11.90	**<0.01**
Water		31.4%	40.2%	10.07	**<0.01**
Salinity	Allocation at later stage	17.4%	22.3%	4.62	**0.02**
Water × Salinity		29.4%	37.6%	9.16	**<0.01**

FIGURES
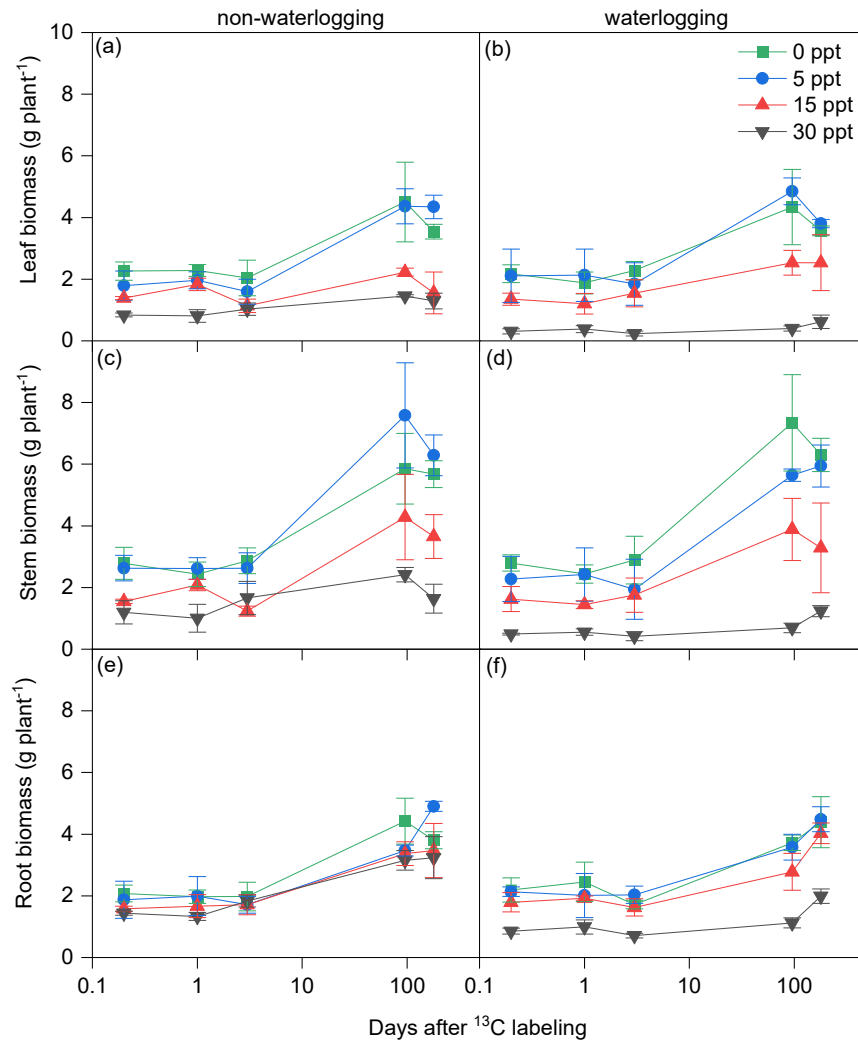
Fig. 1. Plant biomass (mean ± SD, *n* = 4) of different *P. australis* organs (leaves, stems, roots) under different waterlogging (non-waterlogging *vs.* waterlogging) and salinity (0–30 ppt) conditions at day 0, 1, 3, 96, and 150 after ^{13}C labeling. The x-axis is shown as a logarithmic scale.
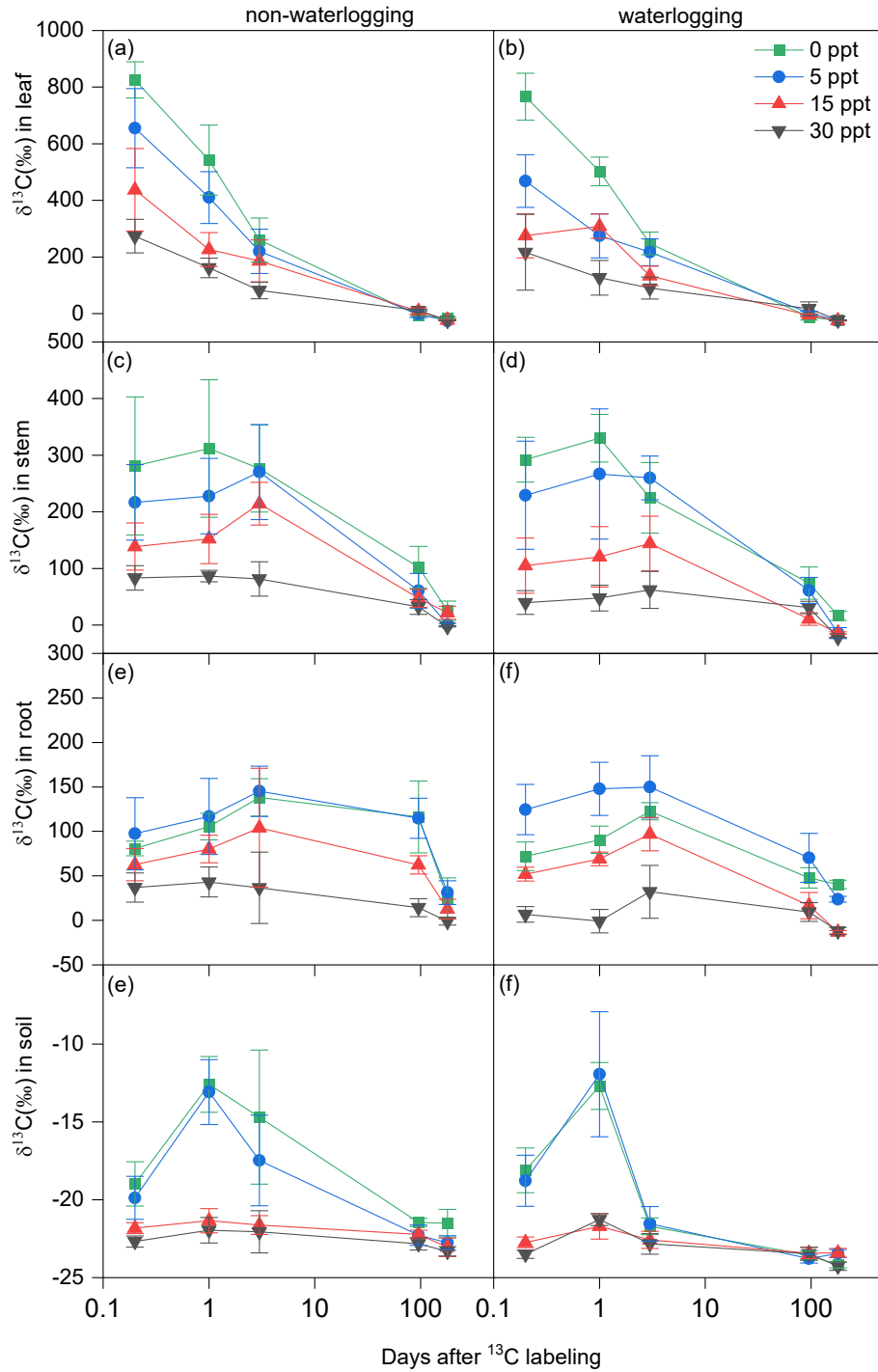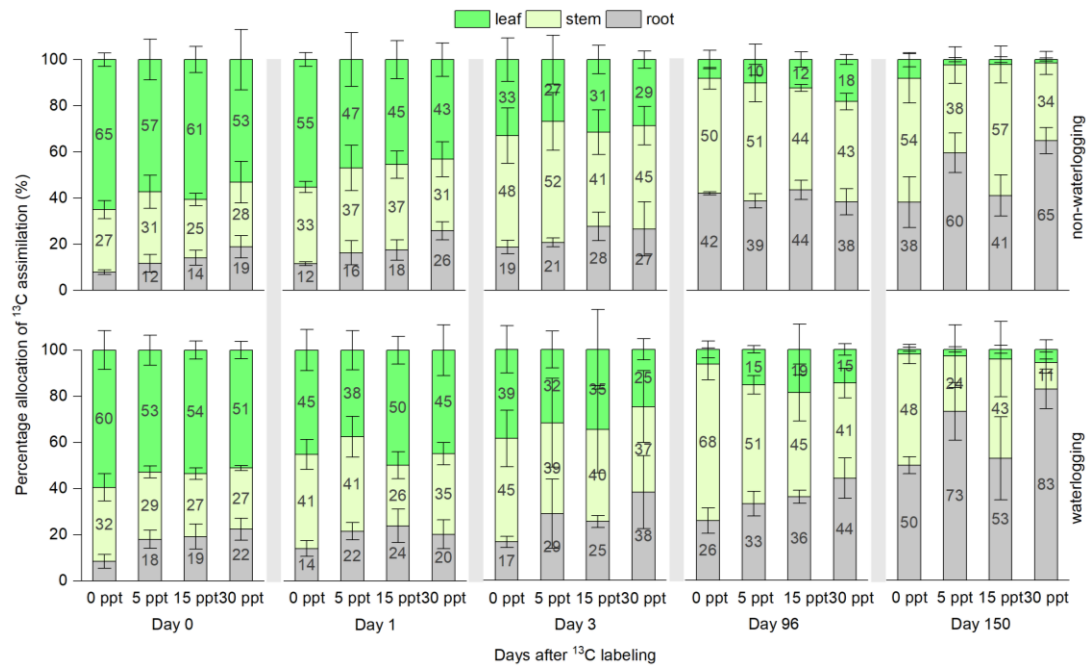
Fig. 2. Temporal changes in δ¹³C values (mean ± SD, $n = 3$) in *P. australis* leaves, stems, and roots under different waterlogging (non-waterlogging *vs.* waterlogging) and salinity (0–30 ppt) conditions at day 0, 1, 3, 96, and 150 after ¹³C labeling. The x-axis is shown as a logarithmic scale.

Fig. 3. Mean percentage of ^{13}C allocation ($^{13}C_{organ}$%) into different plant organs under different waterlogging (non-waterlogging *vs.* waterlogging) and salinity (0–30 ppt) conditions at day 0, 1, 3, 96, and 150 after ^{13}C labeling. The percentage values were calculated using data in Fig. S1. Note: values below 10% are not shown.
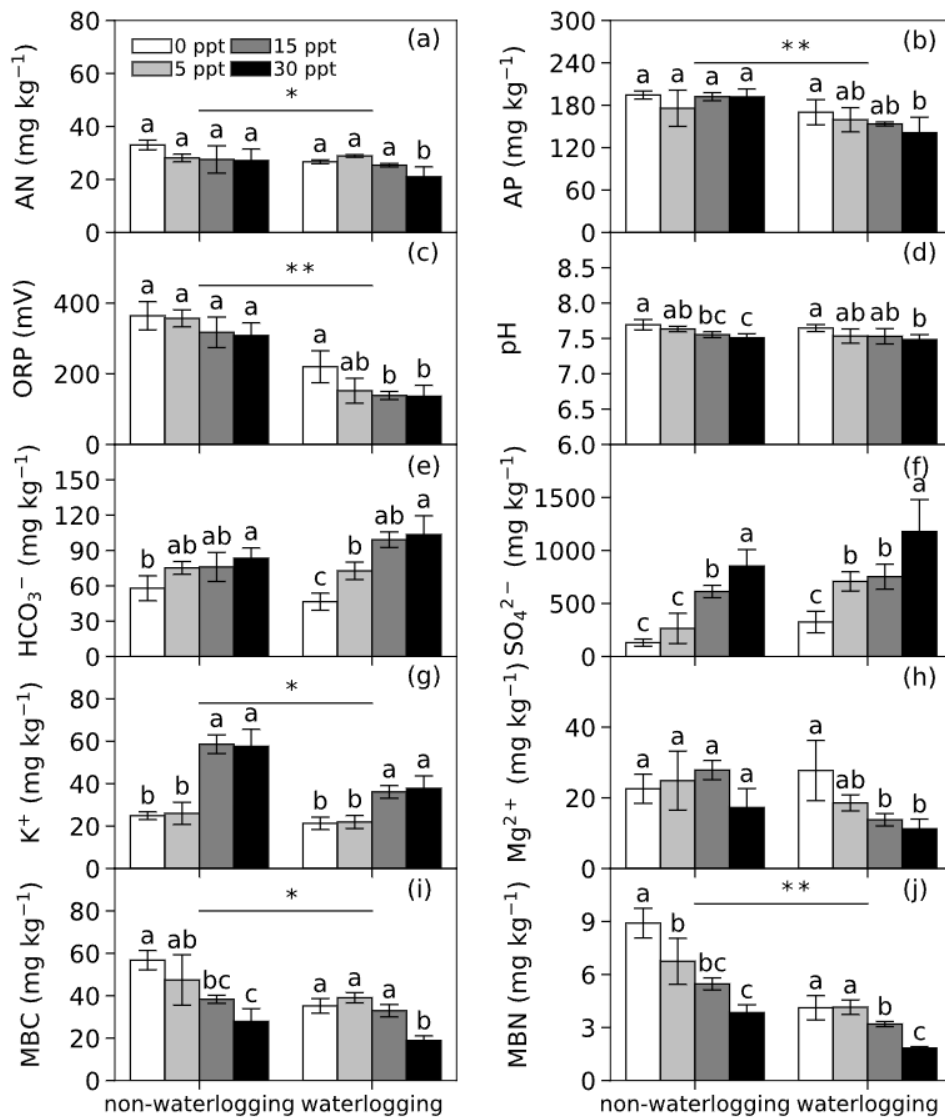
Fig. 4. Edaphic variables, including nutrients, physiochemistry and microbial biomass (mean ± SD; n = 3), under different waterlogging (non-waterlogging $vs.$ waterlogging) and salinity (0–30 ppt) conditions. Different letters indicate significant differences ($P < 0.05$) in the variables among salinity levels. The asterisks above the horizontal lines indicate significant differences (* $P < 0.05$; ** $P < 0.05$) between water table groups (on the average of salinity levels). AN: available nitrogen; AP: available phosphorus; ORP: oxidation-reduction potential; HCO_3^-: bicarbonate ion; SO_4^{2-}: sulfate ion; K^+: potassium ion; Mg^{2+}: magnesium ion; MBC: microbial biomass carbon; MBN: microbial biomass nitrogen.

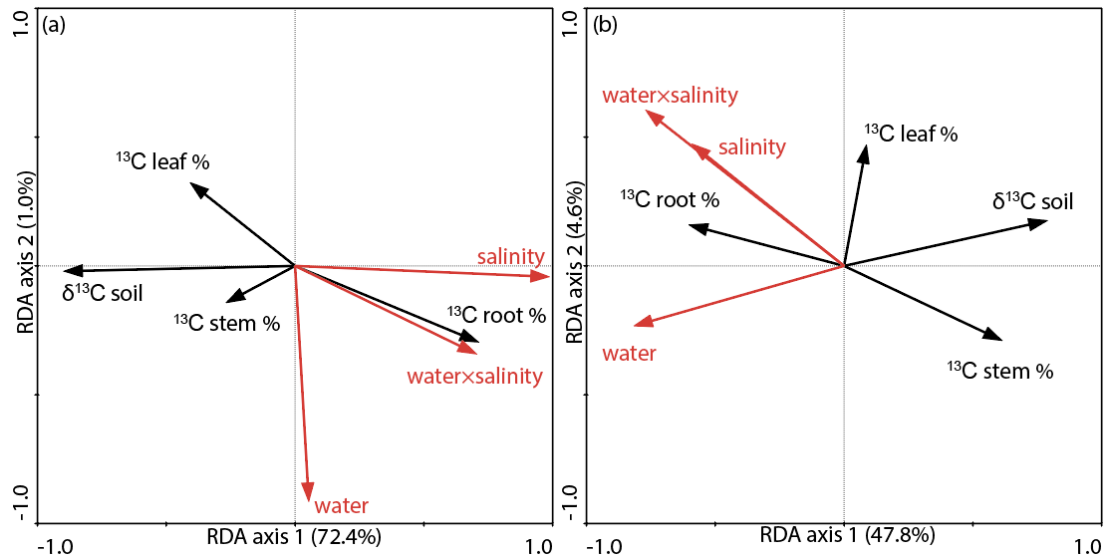**Fig. 5.** Ordination diagram based on redundancy analysis (RDA) of the percentage of ^{13}C allocation ($^{13}C_{organ}$%) within plant and soil $\delta^{13}C$ (black arrows) with respect to treatments (red arrows) of waterlogging (water), salinity and their interactions in early (a) and later growing periods (b).